JOURNAL OF GEOPHYSICAL RESEARCH, VOL. 96, NO. D9, PAGES 17,297–17,305, SEPTEMBER 20, 1991

Global Average Ozone Change From November 1978 to May 1990

J. R. HERMAN, R. MCPETERS, AND R. STOLARSKI

Laboratory for Atmospheres, Goddard Space Flight Center, Greenbelt, Maryland

D. LARKO

ST Systems Corporation, Lanham, Maryland

R. HUDSON

Department of Meteorology, University of Maryland, College Park

A recent recalibration and reprocessing of the total ozone mapping spectrometer (TOMS) data have made possible a new determination of the global average (69°S to 69°N) total ozone decrease of 3.5% over the 11-year period, January 1, 1979, to December 31, 1989, with a 2σ error of 1.4%. The revised TOMS ozone trend data are in agreement, within error limits, with the average of 39 ground-based Dobson stations and with the world standard Dobson spectrometer 83 at Mauna Loa, Hawaii. Superimposed on the 11-year ozone trend is a possible solar cycle effect, quasi-biennial oscillation (QBO), annual, and semiannual cycles. Using solar 10.7-cm flux data and 30-mbar Singapore wind data (QBO), a time series has been constructed that reproduces the long-term behavior of the globally averaged ozone. Removal of the apparent solar cycle effect from the global average reduces the net ozone loss to 2.66 ± 1.4% per decade. The precise value of the global average ozone trend depends on the latitude range selected, with ranges greater than ±69° emphasizing the larger variations at high latitudes.

INTRODUCTION

High-resolution global mapping of the total ozone amount has been obtained from the total ozone mapping spectrometer (TOMS) on the Nimbus 7 satellite since October 1978 [*Klenk et al.*, 1982; *Fleig et al.*, 1983, 1986; *Cebula et al.*, 1988]. An accurate measure of the long-term trend in atmospheric ozone amount is needed to distinguish natural cyclic effects from anthropogenic influences. An examination of previously archived TOMS data (version 5) showed that there were errors in key assumptions used to determine the instrument's long-term calibration [*Hudson et al.*, 1989; *Herman et al.*, 1990, 1991]. These errors led to an estimate of the 69° global average (69°S to 69°N) ozone decrease of about 9.8% between November 1978 and November 1989 [see *Bowman*, 1988]. In this work we show that the actual net decrease is much smaller, and there is good evidence of at least a partial recovery during the years 1986–1990 (possibly due to solar cycle effects). A time series is constructed that represents the relative importance of linear trends, solar cycle effects, and the atmospheric quasi-biennial oscillation (QBO) effects. We briefly discuss some of the errors in the original TOMS data and the means used to correct them. The effects of including the polar regions on the estimated global average ozone trend are also considered.

DESCRIPTION OF THE RECALIBRATED TOMS DATA

TOMS makes measurements of the Earth's radiance in six fixed wavelength channels at 312.5, 317.5, 331.2, 339.8, 360, and 380 nm from a sun-synchronous noontime orbit. The six radiances are measured at each of 35 cross-track positions to cover the regions between the orbital paths (the 35 cross-track scans are completed in 8 s). At least once per day, TOMS measures the solar irradiance by exposing a ground aluminum diffuser plate to the sun in front of the first optical element of the spectrometer. If the reflectivity of the diffuser plate is known as a function of time, then the radiance-irradiance ratio are determined (directional albedo A_m) independent of the spectrometer's sensitivity [*Herman et al.*, 1990, 1991].

Logarithms of ratios of wavelength pairs of directional albedos are formed, N_m, to reduce the effect of atmospheric aerosol scattering, errors in absolute reflectivity of the ground, and the diffuser plate reflectivity. The values of N_m can be converted into ozone amounts by comparison with precomputed tables obtained from solutions of a radiative transfer equation including effects of ozone absorption and multiple Rayleigh scattering [*Dave*, 1966; *Klenk et al.*, 1982].

Errors in the wavelength dependence of the diffuser plate reflectivity result in the various wavelength pairs yielding different ozone trends. By combining the zonally averaged equatorial results from two pairs of wavelengths (described in detail by *Herman et al.* [1991] and requiring that the calculated change in ozone $\Delta\Omega$ is the same value, a correction to the assumed diffuser plate reflectivity E_x can be obtained. Once the correction is obtained as a function of time and wavelength, it can be applied to the entire set of TOMS albedo measurements A_m. Other smaller corrections were applied to the data to minimize the uncertainty in the calculated (version 6) TOMS ozone trend. These include the removal of sea glint data from the calculation of the lower boundary reflectivity determination, a small spacecraft roll error correction, and a procedure for minimizing errors from

Paper number 91JD01553.
0148-0227/91/91JD-01553$05.00

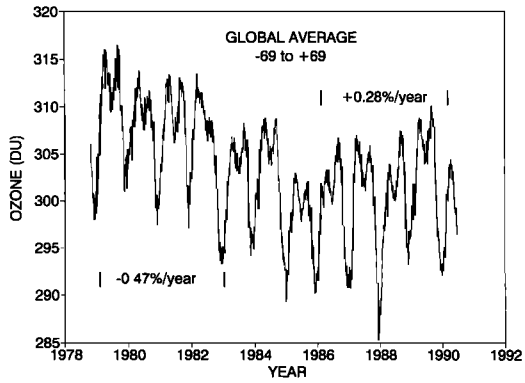

Fig. 1. The area-weighted 69° global average ozone change (−69° to +69° latitude) computed from the TOMS recalibrated ozone data. A linear least squares fit to the data gives a 2.9% decrease from October 1978 to May 1990. Most of the change arising from the recalibration of TOMS occurs after 1984 when the error in the estimated diffuser plate reflectivity began to increase.

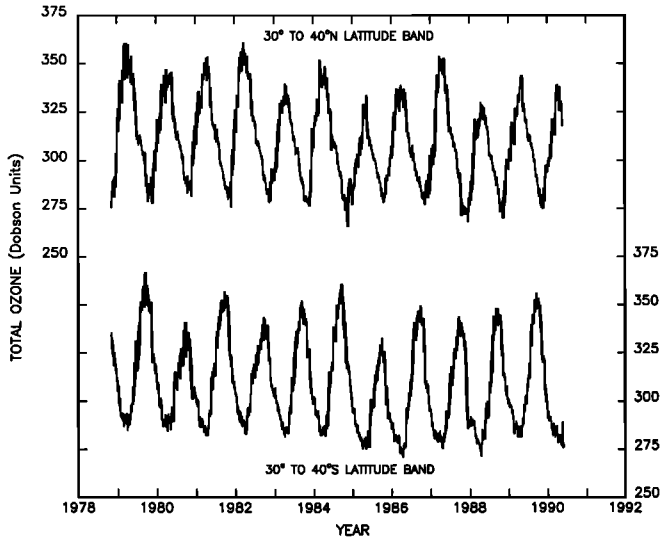

Fig. 2. The zonally averaged ozone data for the 30°–40° northern and southern latitude bands showing the phase and amplitude differences.

occasional chopper wheel synchronization problems with the photon counting electronics.

The version 6 ozone data set is available from the National Space Science Data Center, or zonally averaged subsets of this data are available from the author.

TOMS Global Average Ozone Trend

The ozone data calculated from the TOMS directional albedo measurements can be assembled into nearly continuous maps covering most of the Earth's sunlit surface. Global averages of ozone behavior are calculated from 2° wide zonal averages for latitudes between 69°S and 69°N. Each daily global average is the sum of individual zonal averages weighted by the fractional area of the Earth's surface covered by each zone. The ±69° latitude limitation was selected to eliminate the large regions where no measurements are taken during the extended winter polar darkness.

The 69° global average time dependence from the corrected version 6 ozone data are shown in Figure 1. The double-peaked annual cycle maxima in the TOMS 69° global average ozone results from phase and amplitude differences between the combined northern and southern hemisphere data (for example, see Figure 2). Figure 2 clearly shows the 30°–40° southern hemisphere annual ozone maxima nearly coinciding with the 30°–40° northern hemisphere ozone minima. If the ozone data in Figure 2 are combined (summed), the relative amplitudes of the ozone variation and the phase difference produce a figure similar in appearance to Figure 1.

In the 69° global average the first maximum in each annual cycle is from the northern hemisphere, and the second from the southern hemisphere, with the northern hemisphere peak usually larger during the period 1978–1986 (it is reversed in 1983). After 1986 the second peak is higher on alternate years. Examination of the southern and northern hemisphere zonal average ozone data shows different seasonal behavior in different latitude zones. This occasionally pushes the southern latitude maxima above the northern.

The cyclic behavior of the area weighted 69° global average is similar to the average of the 40°–60° latitude bands. This results from area weighting emphasizing lower latitudes combined with the larger amplitudes that occur at high latitudes.

Using the 69° global average ozone data as shown in Figure 1, a simple estimate of the long-term trend can be obtained from linear least squares fits to the monthly averages for each year (see Table 1). The 69° global average 11-year trend for all months was −1.0 DU/yr, with a variance of ±0.12 DU/yr. Using the 12-month average ozone value for 1979, 311.36 DU (see Table 2), the total percentage decrease over the 11-year period from January 1, 1979, to December 31, 1989, is about 3.5%, with a 2σ error of ±1.4%. The largest component of the ±1.4% uncertainty is in the diffuser plate reflectivity (±1.1%) calculation [*Herman et al.*, 1991]. Part of the uncertainty (±0.25%) arises from the determination of the lower boundary (ground or cloud) reflectivity and an instrumental problem (±0.6%) with synchronizing the entrance slit chopper wheel and the photon counting electronics. An additional uncertainty (±0.4%)

TABLE 1. Average Monthly Ozone Decrease for Four Latitude Limits

	Ozone Decrease, DU/yr											
Latitude	Jan.	Feb.	March	April	May	June	July	Aug.	Sept.	Oct.	Nov.	Dec.
61°	1.0	0.91	0.86	0.82	1.0	0.93	0.72	0.60	0.60	0.89	0.92	1.0
65°	1.0	0.95	0.92	0.91	1.1	1.0	0.79	0.66	0.71	0.99	1.0	1.1
69°	1.1	0.97	0.98	0.99	1.2	1.1	0.85	0.73	0.81	1.1	1.1	1.1
89°	1.1	0.96	1.1	1.1	1.2	1.1	0.90	0.92	1.1	1.2	1.2	1.2

TABLE 2. Annual Average Ozone Amount From the 69° Global Average

Year	Ozone Amount, DU
1979	311.36
1980	309.06
1981	309.05
1982	307.28
1983	303.07
1984	303.83
1985	298.76
1986	300.76
1987	300.90
1988	301.19
1989	303.97
1990	298.83

TABLE 3. The Effect of Latitude Range on Global Average Ozone Trend

Latitude Range	Trend,* %/yr 1979–1983	Trend,* %/yr 1986–1990	O_3 Trend,† % 1979–1990
±61°	−0.37	+0.36	−3.02
±65°	−0.42	+0.30	−3.28
±69°	−0.47	+0.28	−3.54
±89°‡	−0.56	+0.19	−3.85

*The trend numbers are computed from a least squares fit to the data starting and ending at the respective minimum near the specified year.

†The 11-year percent change in ozone is computed form 11-year changes for each month, as shown in Table 1.

‡Includes only sunlit grid points.

arises from the statistical methods used in determining the trend [*Stolarski et al.*, 1991], increasing the overall uncertainty to ±1.4%. Slightly different trend numbers can be obtained using different methods of averaging the ozone data. A procedure based on removing the average seasonal variation is discussed later.

The 69° global average ozone trend derived from a least squares fit to the annual averages shown in Table 2 is −3.53% for the 1979–1989 period. The small difference (0.03%) between the trend calculated from Table 1 data and Table 2 data arises from the least squares fitting to a small number of points. The 1990 annual average shown in Table 2 has a slightly larger error than the preceding years because of increased chopper synchronization errors after May 1990.

During the first 4 years after initial TOMS data (November 1, 1978), the annual 69° global average amount of ozone decreased at a nearly uniform rate of 0.47% per year. This was followed by a sharp decrease in 1983 and an ozone minimum in mid-1985 (the maximum value in 1985 is 4.4% below the maximum in 1979). The 1983 and 1985 minima appear to be related to QBO effects [*Bojkov*, 1987]. Since 1986 there has been a gradual increase in the 69° global average amount of ozone at a rate of about 0.28% per year.

The current data set encompasses a little over 11 years (November 1978–May 1990) and appears to include possible solar cycle effects. However, additional ozone data are needed before a physical relationship can be established with the 11-year 10.7-cm solar cycle data (F10.7) [*Bojkov et al.*, 1990; *Stolarski et al.*, 1991]. The last data included in Figure 1 are from May 1990. The last annual average in Table 2 is based on the entire year of 1990. In June 1990, TOMS developed chopper wheel synchronization problems that may make future ozone trend data questionable at the 1 to 2% level of uncertainty. Continuation of a comparable ozone trend analysis may require using data from other satellites (e.g., the solar backscattered ultraviolet, SBUV/2, series of ozone-observing spectrometers). Since September 1990, the TOMS instrument has partially recovered to about a 20% incidence of chopper wheel synchronization errors (down from a maximum of 80%).

The Effect on Trends of Including High-Latitude Data

The global average ozone trend computed from TOMS data includes only daylight regions. Because the largest ozone changes are observed near the poles, with almost no change near the equator [*Stolarski et al.*, 1991], the calculated value is sensitive to the specific latitude range used for the ozone trend. Computing global ozone averages that include TOMS data above 69° latitude are complicated because nighttime data are missing during the winter months. There are two possible ways of including these data in the global average: (1) to fill in the missing data with the value of the last daytime ozone data point at the nearest latitude or (2) to only include daytime data in the average and adjust the area weighting to include just the sunlit portions of the globe.

Only the second case is considered, since in both cases the main results are similar. The amplitudes of the seasonal peaks are increased, and the amplitude of the second annual peak is reduced relative to the first peak. This shows the dominance of the north polar seasonal ozone variation over the south polar data in the computation of the seasonal time dependence of the global average ozone. Using the high-latitude data, the rate of ozone decrease from 1978 to 1983 is increased to 0.56% per year, and the recovery rate between 1986 and 1990 is reduced to 0.19% per year (see Table 3). The net decrease over 11 years is 3.85%. Inclusion of polar daylight regions in the global average (89° global average) yields an additional 0.31% decrease relative to the 69° global average (see Table 3). The overall effect of the south polar ozone hole on global average trends is probably much larger than might be expected from its relatively small area and time duration. This is because of the global redistribution of ozone filling in the hole when the south polar vortex weakens each November.

Analysis of Global 69° Average Time Series

The major features of the 11-year ozone time series (shown in Figure 1) can be decomposed into components of the linear long-term trend, QBO effects, and solar cycle effects. This section presents a qualitative derivation of the possible major components contributing to the ozone time series. The resulting time series terms are comparable to a statistical model derivation [*Stolarski et al.*, 1991] of an ozone trend time series.

The following steps were taken to successively derive the time series terms from the ozone data shown in Figure 1.

1. An average seasonal cycle was obtained by averaging the ozone amount from each day of the year over the 11-year data set $F(t)$. The resulting annual cycle was repeated to

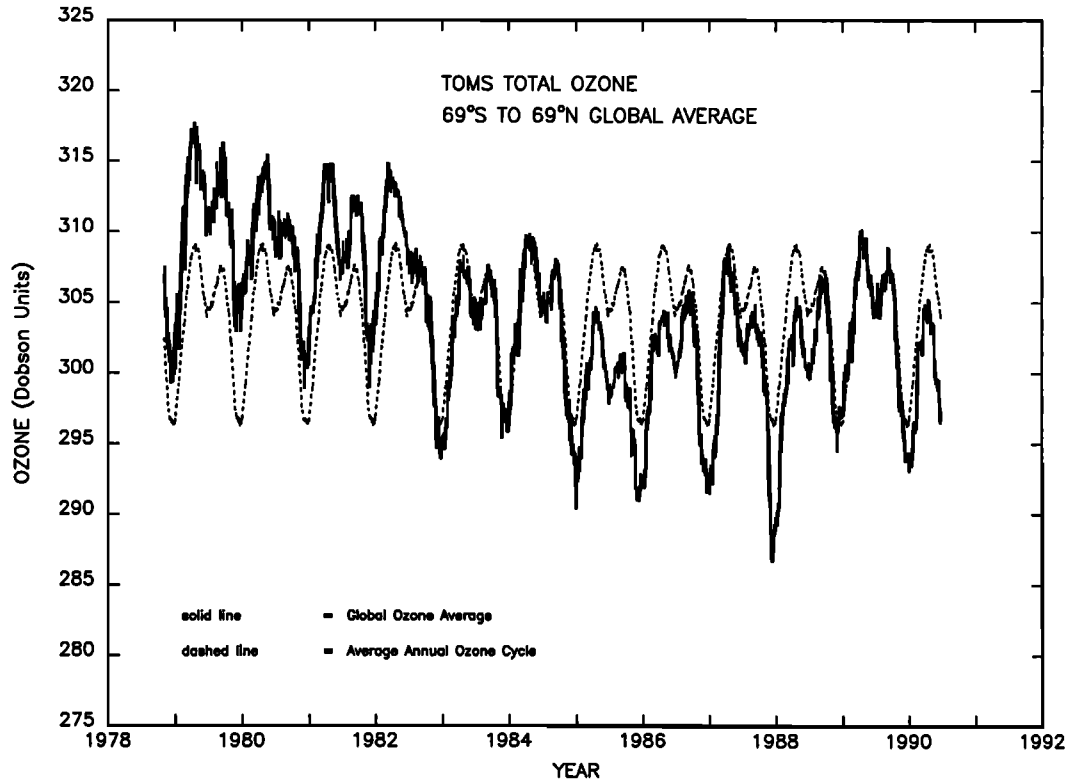

Fig. 3. The 11.5-year 69° global average ozone variation $F(t)$ and the average annual variation extended over the 11.5-year period, $A(t)$.

span the data (see $A(t)$, shown by the dashed curve in Figure 3).

2. Form the percent difference,

$$D_{FA}(t) = 100[F(t) - A(t)]/A(t), \quad (1)$$

to remove the average seasonal behavior. Fit $D_{FA}(t)$ using linear least squares to obtain $L_{FA}(t)$, as shown in Figure 4. The slope of $L_{FA}(t)$ is -0.32% per year.

3. Remove the overall linear trend from $D_{FA}(t)$ by forming the quantity

$$S(t) = D_{FA}(t) - L_{FA}(t), \quad (2)$$

as shown in Figure 5. $S(t)$ still has possible solar cycle and QBO effects that can be removed if they are correlated with the standard indices (F10.7 for the solar cycle and the 30-mbar Singapore winds for the QBO effect).

4. Model calculations [*World Meteorological Organization* (*WMO*), 1990, chapter 7] have predicted an 11-year solar cycle ozone variation of between 0.7 and 2.0% from maximum to minimum. $S(t)$, in Figure 5, suggests such a correlation because ozone is higher during the solar maximum periods at the beginning and end of the 11 years than it is in the middle during solar minimum. The 10.7-cm solar radio flux [*Bojkov et al.*, 1990] has been used for many years as a surrogate for the ultraviolet solar cycle variation that produces (and dissociates) ozone. The F10.7-cm solar flux has been compared to the Nimbus 7 SBUV 205-nm solar flux (November 1978–mid-1982) during the period when the original SBUV diffuser plate reflectivity calibration was valid [*Donnelly and Heath*, 1985; *Herman et al.*, 1990]. During this limited period around solar maximum the overall shape of the 205-nm flux was matched by the 10.7-cm flux.

Using F_{avg}, the average value of $F_{10.7}(t)$ over the entire 11-year data record, form the fractional deviation

$$D_{10.7} = [F_{10.7} - F_{avg}]/F_{avg}. \quad (3)$$

$S(t)$ is then fit with $mD_{10.7}(t)$ by finding the value of m (m = 1.55) that minimizes the least squares difference between the two functions (see Figure 6). The results are consistent with the predicted strong correlation between solar cycle ultraviolet flux variation and the corresponding ozone variation.

5. In order to remove the solar variation from $S(t)$, form

$$Q'(t) = S(t) - mD_{10\,7}, \quad (4)$$

as shown in Figure 7. $Q'(t)$ shows a strong QBO effect along with a residual trend of $+0.54\%$ per decade. The residual trend in (4) occurs because the F10.7 cycle is not symmetric about its midpoint. If the residual trend formed by a least squares fit, $L_{Q'}(t)$, (shown as the dashed curve in Figure 7) is subtracted from $Q'(t)$ to form

$$Q(t) = Q'(t) - L_{Q'}(t), \quad (5)$$

then $Q(t)$ can be compared with the QBO wind function on the basis of the 30-mbar Singapore winds. Summarizing (3)–(5) for $Q(t)$ gives

$$Q(t) = F(t) - A(t) - L_{FA}(t) - 1.55D_{10.7} - L_{Q'}(t), \quad (6)$$

where

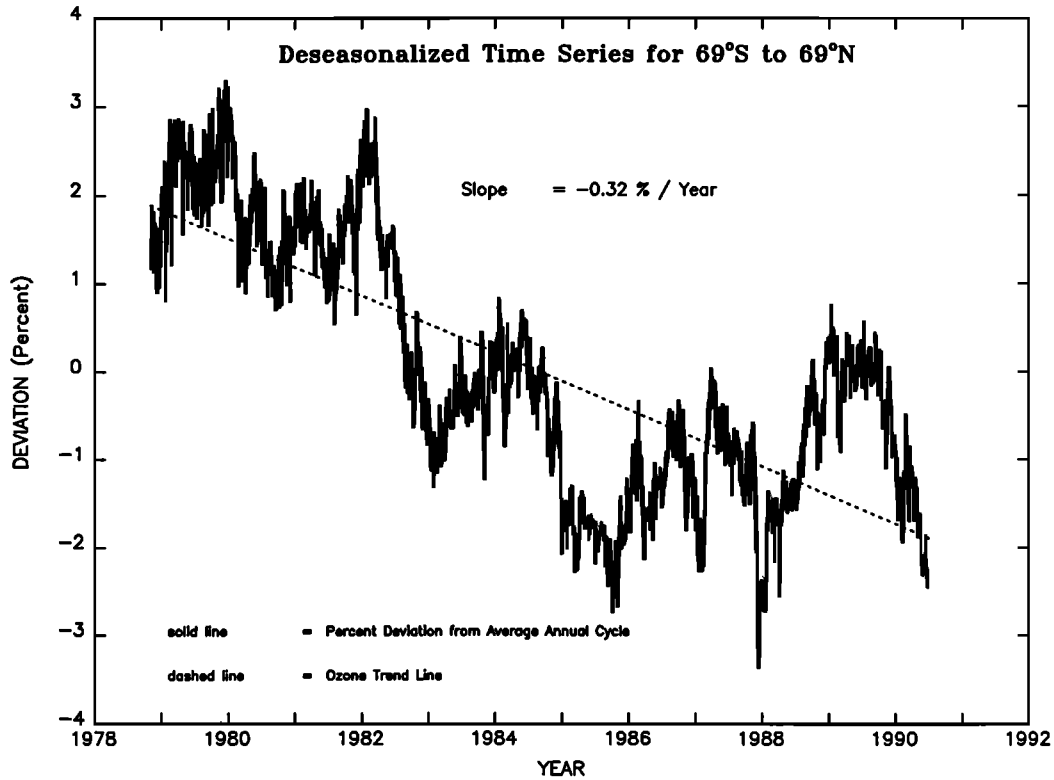

Fig. 4. The fractional difference, $D_{FA}(t) = [F(t) - A(t)]/A(t)$, and the linear least squares fit, $L_{FA}(t)$, with a slope of −0.32% per year.

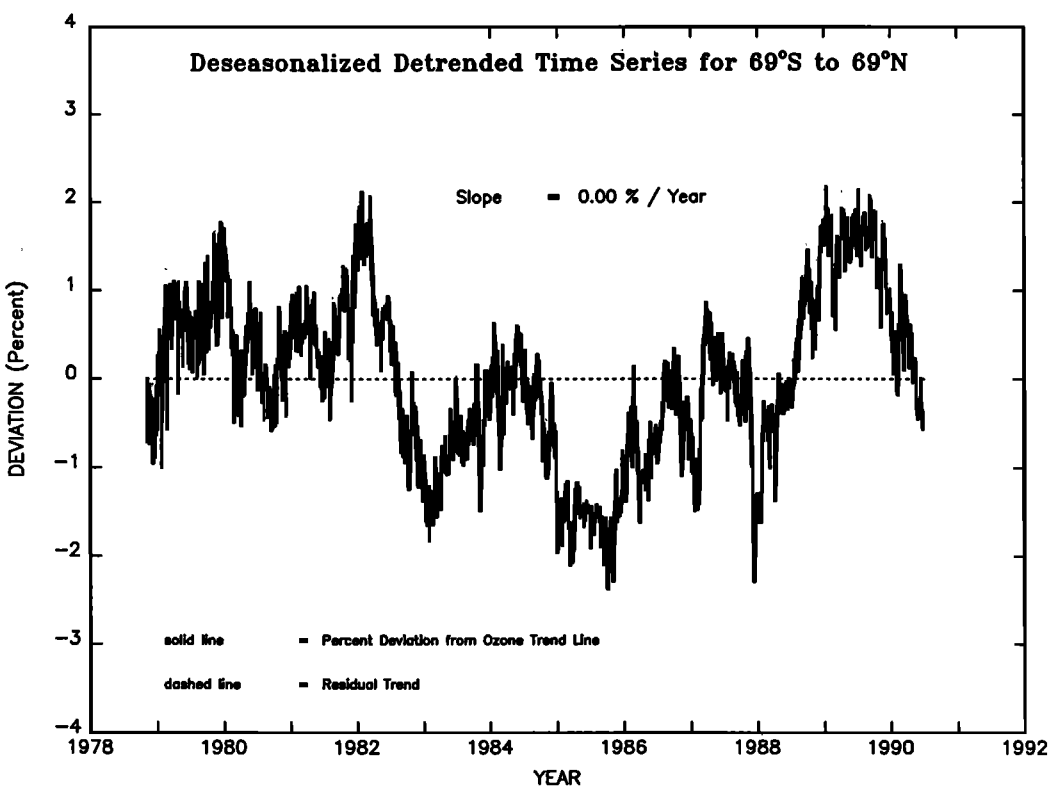

Fig. 5. The fractional ozone change $S(t)$ after the overall 11-year trend and seasonal effects are removed.

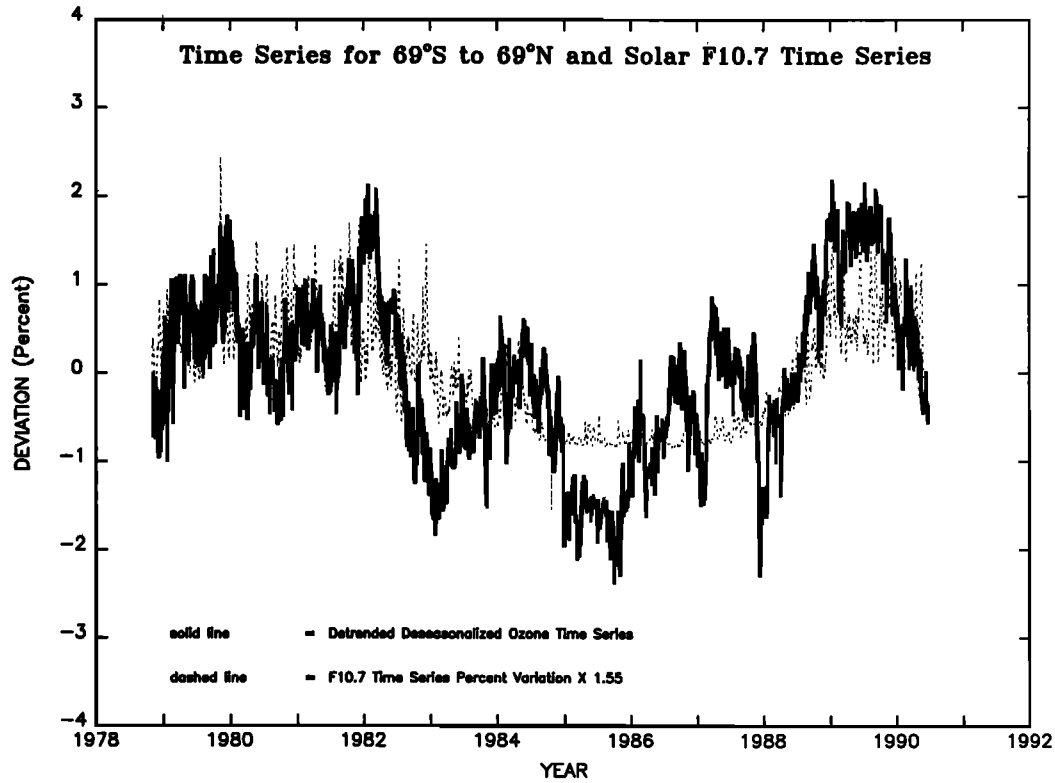

Fig. 6. A comparison of $S(t)$ with $D_{10.7}$, the scaled variation in the 10.7-cm solar flux, about its average value. The scaling factor is $m = 1.55$ for the least squares fit between S and D.

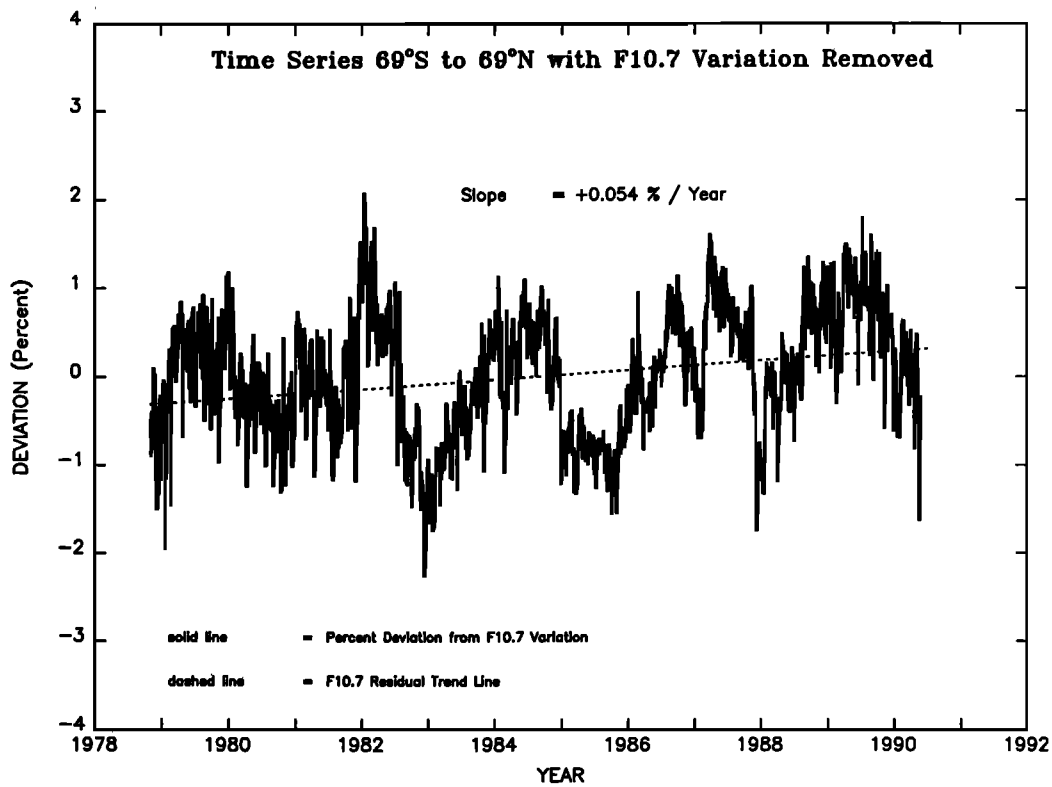

Fig. 7. The difference $Q'(t)$ between $S(t)$ and $D_{10.7}$. The least squares fit $L_{Q'}(t)$ to $Q'(t)$ shows the residual trend that may be associated with solar cycle asymmetry of the starting and stopping points of the F10.7 data set.

$F(t)$ the original daily values of globally averaged ozone;
$A(t)$ = the average seasonal ozone variation over 11 years;
$L_{FA}(t)$ the least squares fit to $S(t) = [F(t) - A(t)[/A(t)$;
$D_{10.7}(t) = [F_{10.7}(t) - F_{avg}]/F_{avg}$;
F_{avg} the 11-year average of the 10.7-cm solar flux, $F_{10.7}(t)$;
$L_{Q'}(t)$ least squares fit to $Q'(t) = S(t) - mD_{10.7}$.

6. The quasi-biennial oscillation (QBO) of the tropical winds in the lower stratosphere (30 mbar) can be represented by the Singapore wind data obtained from J. Angell (private communication, 1990) and *Lait et al.* [1989]. Measurements of the wind velocity $W(t)$ show a nearly square wave behavior with time, first in one direction for about a year and then quickly reversing for the second year (see the lower half of Figure 8). The deviation of the QBO winds from their 11-year average W_{avg} is formed with reversed sign:

$$D_W(t) = [W_{avg} - W(t)]/W_{avg}, \quad (7)$$

to adjust the phase with respect to the ozone data $Q(t)$. If $D_W(t)$ is averaged with a 1-year running average, the result, $\langle D_W(t)\rangle$, is a nearly sinusoidal function. Here $k\langle D_W(t)\rangle$ is shown in Figure 8 as the dashed curve (with $k = 0.28$), where the magnitude of k has been adjusted to give the best fit to $Q(t)$. The residuals are a few tenths of a percent. The original winds data, $D_W(t)$, shown in the lower half of Figure 8, fit $Q(t)$ with even smaller residuals than $\langle D_W(t)\rangle$. $Q(t)$ appears to follow $D_W(t)$ in both phase and in the shape of its amplitude.

7. A smoothed fit $D_{sf}(t)$ to the original deseasonalized ozone time series $D_{FA}(t)$ can be formed by reversing the construction of $Q(t)$ using the QBO winds function $0.28\langle D_W(t)\rangle$:

$$D_{sf}(t) = L_{Q'}(t) + L_{FA}(t) + 1.55D_{10.7} + 0.28\langle D_W(t)\rangle, \quad (8)$$

where $L_{Q'}$ and L_{FA} are linear least squares fits to $Q'(t)$ and $D_{FA}(t)$, respectively, and $\langle D_W(t)\rangle$ is the 1-year running average of the deviations from the 11-year mean of the 30 mbar Singapore winds $W(t)$.

$D_{sf}(t)$ is shown by the dashed line in Figure 9. This clearly compares well with $D(t)$, showing that (8) is a reasonable model for statistical analysis of the 69° global ozone average. If the two curves are subtracted, $D(t) - D_{sf}(t)$, the residual trend is not statistically significant (a slope of 0.004% per year), and the difference is within ±1%.

A Fourier transform power spectrum analysis of the ozone data in Figure 8 shows a strong peak with a period of 28.7 ± 0.3 months. The phase of the low-frequency wave in the ozone data shifts slowly with respect to the annually averaged QBO data (see Figure 8). The phase relationship depends on the relative contributions to the globally averaged ozone variations from the different latitude bands. The equatorial ozone variation is in phase with the 30-mbar Singapore winds, while the 50° latitude variation is approximately 180° out of phase.

DISCUSSION

The results represented by (8) are very suggestive of a direct correlation between the 11-year 69° global average ozone trend and the 11-year solar cycle. Such an interpretation must be considered cautiously, since the TOMS ozone data span only one solar cycle. The apparent solar cycle response of ozone is about 1.5% from minimum to maximum (see Figure 6), consistent with the model predictions of 0.7–2.0% [*WMO*, 1990, chapter 7].

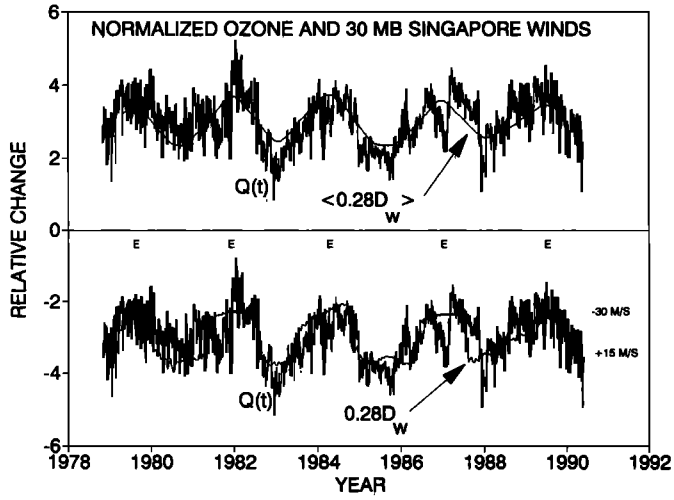

Fig. 8. Comparison of the ozone variation $Q(t)$, after seasonal, long-term, and solar cycle changes are removed, with the scaled deviation of the 30-mbar Singapore winds from its average value $\langle D_W(t)\rangle$. The value of the scaling factor, $k = 0.28$, is used to produce a least squares fit between Q and $\langle D\rangle$. Also shown in the lower half are the original winds data compared to $Q(t)$. The maxima E represent easterlies, peaking near 30 m/s, while the minima are westerlies at about 15 m/s. There is a visual suggestion that $Q(t)$ follows both the phase and amplitude shape of $D_W(t)$.

The difference between ozone variation $S(t)$, shown in Figure 6, and $mD_{10.7}$ has a residual trend of +0.54% per decade (see Figure 7). This means that the segment of $F_{10.7}(t)$ data used is slightly asymmetric over the 11-year period. The asymmetry is confirmed by a least squares fit to the $F_{10.7}(t)$ fractional difference, $mD_{10.7}(t)$, having a slope of −0.85% per decade. Therefore part of the trend in the 11 years of ozone data may be from the incomplete solar cycle represented in the $F10.7$-cm data. If the solar cycle effect on ozone is assumed to be real, then the true long-term ozone decrease is 3.2 − 0.54 = 2.7 ± 1.4% per decade. This is consistent with a linear trend of 2.6 ± 1.4% per decade deduced from a statistical study of the same data [*Stolarski et al.*, 1991], which simultaneously solved for the trend and solar cycle effects.

A recent analysis of total ozone data obtained from a set of 39 well-calibrated ground-based Dobson spectrometer stations shows that the current TOMS ozone trend recalibration agrees within error limits with the Dobson trends [*Komhyr et al.*, 1989; *McPeters and Komhyr*, 1991; *Herman et al.*, 1991]. The data used for comparison were obtained by sampling the TOMS data set for coincidences with Dobson measurements in time and location. An additional comparison with TOMS ozone data was made using coincident data from the world standard Dobson spectrometer 83 obtained during its repeated calibrations at Mauna Loa, Hawaii. As with the average of 39 stations, the TOMS-Dobson trend comparison was within experimental error but with much greater variance.

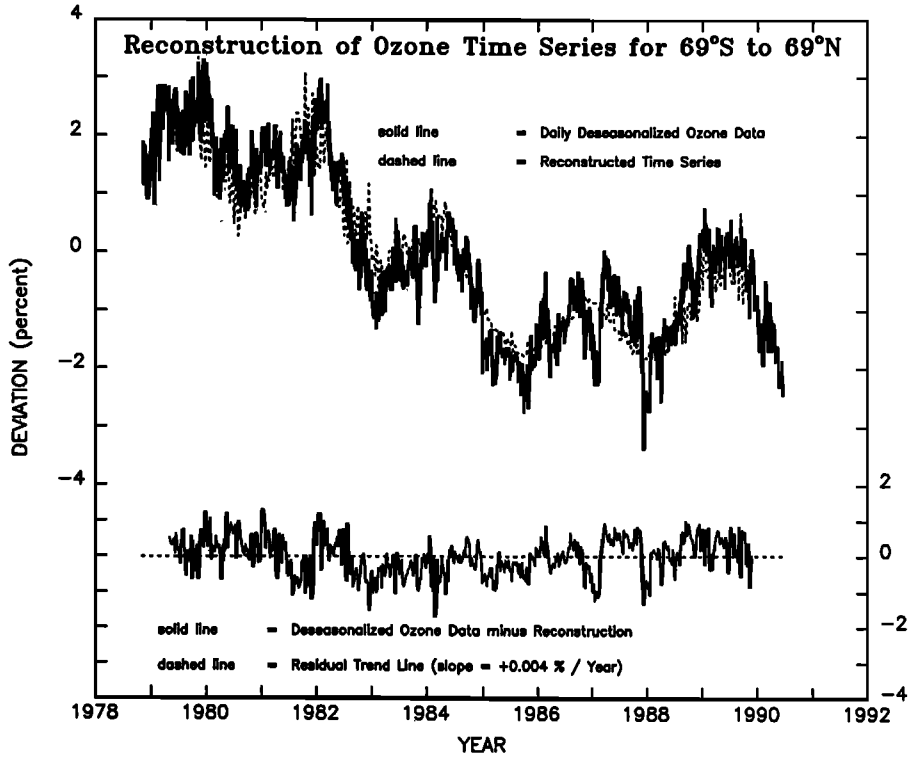

Fig. 9. The reconstruction of the fractional ozone trend $D_{sf}(t)$ from (8), compared with original deseasonalized ozone data $D_{FA}(t)$ from (1). The lower half is the difference, $D_{FA}(t) - D_{sf}(t)$, between the original deseasonalized ozone data and the reconstruction.

Conclusion

Recalibration of the TOMS directional albedo data has led to a much smaller ozone trend than the previously archived (version 5) data. As shown in Figure 1, the 69° global average ozone trend is not linear. Instead, it first decreases at a rate of about 0.47% per year (1979–1983), shows irregular behavior with a net decrease (1983–1985), and then has a moderate rate of increase of about 0.28% per year (1986–1990). Using monthly averages, the net change over the 11-year data record is −3.54 ± 1.4% (−0.32% per year). Linear least squares fitting to the entire 11.5-year deseasonalized ozone trend data set (see Figure 4) also shows a net change of −3.52 ± 1.4% for 11 years (−0.32% per year). The observed global average ozone data suggests a correlation with the 11-year solar cycle superimposed on a net overall decrease in ozone amount. If the apparent solar cycle correlation represents a true physical effect, then the net ozone loss in the atmosphere is 3.2 − 0.54 = 2.66 ± 1.4% per decade. However, the length of the data record (11.5 years) is insufficient to be certain of the physical relationship with solar ultraviolet activity. In addition to the solar cycle effect there appears to be a QBO component in the global average ozone data, of period 28.7 ± 0.3 months, that is approximately 180° out of phase with the 30-mbar Singapore winds.

Comparison with ozone data obtained from an average of 39 Dobson spectrometer stations and from the world standard Dobson spectrometer 83 shows that the TOMS (version 6) and Dobson ozone trends agree within experimental error.

References

Bojkov, R., The 1983 and 1985 anomalies in ozone distribution in perspective, *Mon. Weather Rev.*, *115*, 2187–2201, 1987.

Bojkov, R., L. Bishop, W. J. Hill, C. Reinsel, and G. C. Tiao, A statistical analysis of revised Dobson total ozone data over the northern hemisphere, *J. Geophys. Res.*, *95*, 9785–9808, 1990.

Bowman, K. P., Global trends in total ozone, *Science*, *239*, 48–50, 1988.

Cebula, R. P., H. Park, and D. F. Heath, Characterization of the Nimbus-7 SBUV radiometer for the long-term monitoring of stratospheric ozone, *J. Atmos. Oceanic Technol.*, *5*, 215–227, 1988.

Dave, J. V., Multiple scattering in a non-homogeneous, Rayleigh atmosphere, *Meteorol. Monogr.*, *7*, 29, 1966.

Donnelly, R. F., and D. F. Heath, Solar uv radiation variations and their stratospheric and climatic effects, *Adv. Space Res.*, *5*, 145–148, 1985.

Fleig, A. J., D. F. Heath, K. F. Klenk, N. Oslik, K. D. Lee, H. Park, P. K. Bhartia, and D. Gordon, User's guide for the Solar Backscattered Ultraviolet (SBUV) and the Total Ozone Mapping Spectrometer (TOMS) RUT-S and RUT-T data sets: October 31, 1978 to November 1, 1980, *NASA Ref. Publ.*, *1112*, 1983.

Fleig, A. J., P. K. Bhartia, C. G. Wellemeyer, and D. S. Silberstein, Seven Years of total ozone from the TOMS instrument—A report on data quality, *Geophys. Res. Lett.*, *13*, 1355–1358, 1986.

Herman, J. R., R. D. Hudson, and G. Serafino, Analysis of the eight-year trend in ozone depletion from empirical models of solar backscattered ultraviolet instrument degradation, *J. Geophys. Res.*, *95*, 7403–7416, 1990.

Herman, J. R., R. Hudson, R. McPeters, R. Stolarski, Z. Ahmad, X.-Y. Gu, S. Taylor, and C. Wellemeyer, A new self-calibration method applied to TOMS and SBUV backscattered ultraviolet data to determine long-term global ozone change, *J. Geophys. Res.*, *96*, 7531–7545, 1991.

Hudson, R. D., J. R. Herman, and G. Serafino, On the determination of long-term trends from SBUV ozone data, in *Ozone in the Atmosphere, Proceedings of the Quadrennial Ozone Symposium 1988 and Tropospheric Ozone Workshops*, edited by R. Bojkov and P. Fabian, pp. 182–192, A. Deepak, Hampton, Va., 1989.

Klenk, K. F., P. K. Bhartia, A. J. Fleig, V. G. Kaveeshwar, R. D. McPeters, and P. M. Smith, Total ozone determination from the

backscattered ultraviolet (BUV) experiment, *J. Appl. Meteorol.*, *21*, 1672–1684, 1982.

Komhyr, W. D., R. D. Grass, and R. K. Leonard, Dobson spectrophotometer 83: A standard for total ozone measurements, 1962–1987, *J. Geophys. Res.*, *94*, 9847–9861, 1989.

Lait, L., M. R. Schoberl, and P. A. Newman, Quasi-biennial modulation of the Antarctic ozone depletion, *J. Geophys. Res.*, *94*, 11,559–11,571, 1989.

McPeters, R., and W. D. Komhyr, Long-term changes in the total ozone mapping spectrometer relative to world primary standard Dobson spectrometer 83, *J. Geophys. Res.*, *96*, 2987–2993, 1991.

Stolarski, R. S., P. Bloomfield, R. D. McPeters, and J. R. Herman, Total ozone trends deduced from Nimbus 7 TOMS data, *Geophys. Res. Lett.*, *18*, 1015–1018, 1991.

World Meteorological Organization, Report of the international ozone trends panel, *Rep. 18*, pp. 499–542, Geneva, 1990.

J. R. Herman, R. McPeters, and R. Stolarski, Laboratory for Atmospheres, Goddard Space Flight Center, Greenbelt, MD 20771.

R. Hudson, Department of Meteorology, University of Maryland, College Park, MD 20742.

D. Larko, ST Systems Corporation, 4400 Forbes Boulevard, Lanham, MD 20706.

(Received April 1, 1991;
revised June 6, 1991;
accepted June 10, 1991.)